Revista Brasileira de Cartografia (2015) N^0 67/7: 1497-1507
Sociedade Brasileira de Cartografia, Geodésia, Fotogrametria e Sensoriamento Remoto
ISSN: 1808-0936

BIO-OPTICAL MODEL TUNING FOR RETRIEVING THE TOTAL SUSPENDED MATTER CONCENTRATION IN BARRA BONITA RESERVOIR

Ajustamento de Modelos Bio-Ópticos para Estimar a Concentração de Sólidos Suspensos Totais no Reservatório de Barra Bonita

Nariane Bernardo[1], Enner Alcântara[1], Fernanda Watanabe[1], Thanan Rodrigues[1], Nilton Imai[1], Marcelo Curtarelli[2], Cláudio Barbosa[2]

[1]São Paulo State University – UNESP
Department of Cartography
305, Roberto Simonsen Street, Presidente Prudente, SP, Brazil, 19060-900
{narianebernardo, ennerha, fernandasyw, twalesza, nilton.imai}@gmail.com

[2]National Institute for Space Research – INPE
Image Processing Division
Avenida dos Astronautas, 1758, 12227-010 - São José dos Campos - SP, Brazil
claudio@dpi.inpe.br

Recebido em 16 de Março, 2015/ Aceito em 25 de Agosto, 2015
Received on March 16, 2015/ Accepted on August 25, 2015

ABSTRACT

The main goal of this work was assessing the potential application of hyperspectral data to estimate the total suspended matter concentration in Barra Bonita Reservoir, São Paulo. The use of remote sensing data is a powerful motoring tool in water quality due to its capability to produce temporal and spatial data. Traditional monitoring techniques do not produce spatial and temporal information properly, and then, remote sensing data can help to overcome this gap. In order to estimate water quality parameters, quantitatively, the bio-optical models can be used to correlate aquatic compounds and water optical spectral properties registered by remote sensors. In situ hyperspectral measurements were used to calibrate and validate the bio-optical models that have already been published, and to create a new empirical model, based on the correlation between the total suspended matter concentration and remote sensing reflectance values. Obtained results were evaluated by using error analysis (Root Mean Squared error - RMSE and Mean Absolute Percentage Error – MAPE, and coefficient of determination - R^2), as well as the use of spectral bands from orbital sensors were also analyzed. The best TSM retrieval model used near infrared region, presented the slightest mistake to estimate suspended solid concentration.

Keywords: Water Monitoring, Inherent Optical Properties, Empirical Algorithms.

RESUMO

O objetivo deste trabalho foi avaliar o potencial de aplicação de dados hiperespectrais em estimar a concentração de sólidos suspensos totais no reservatório de Barra Bonita, em São Paulo. O uso de dados de sensoriamento remoto é uma poderosa ferramenta de monitoramento da qualidade da água, devido a sua capacidade de produzir dados temporais e espaciais. Técnicas de monitoramento tradicionais não produzem informação espacial e temporal periódica adequada e

os dados de sensoriamento remoto podem auxiliar na superação dessa lacuna. Com o objetivo de estimar parâmetros da qualidade da água, de modo quantitativo, podem ser utilizados modelos bio-ópticos que relacionem a concentração de componentes aquáticos e suas propriedades espectrais registradas por sensores remotos. Dados hiperespectrais medidos in situ foram utilizados para calibrar e validar modelos bio-ópticos previamente divulgados na literatura, e gerar um novo modelo empírico, baseado na correlação entre a concentração de sólidos suspensos totais e a reflectância de sensoriamento remoto. Os resultados obtidos foram avaliados por meio de análise de erros (Raiz Quadrada do Erro Médio Quadrático Percentual – RMSE, Erro Médio Absoluto em Porcentagem - MAPE, coeficiente de determinação - R^2). O melhor modelo para estimar as concentrações de sólidos em suspensão utilizou a região espectral do infravermelho próximo, apresentando menor erro de estimativas de sólidos suspensos totais.

Palavras chaves: Monitoramento Aquático, Propriedades Óticas Inerentes, Algoritmos Empíricos.

1. INTRODUCTION

Remote sensing reflectance (R_{rs}) is influenced by environmental parameters, including climate, water system type (bay, estuaries, rivers, lakes, sea and so on), as well as the concentration and characteristics of aquatic substances (GITELSON *et al.*, 1993; ROTTA *et al.*, 2013). Remote sensing is a powerful tool for aquatic systems monitoring, since traditional techniques, such as in situ measurements, do not provide data with spatial and temporal coverage needed to cope with the extreme variability of those environments (TANG *et al.*, 2013).

Several attempts have been made to develop models to retrieve water quality parameters using R_{rs} (GOODIN *et al.*, 1993; ODERMATT *et al.*, 2012), among which the Total Suspended Matter concentration (hereafter, TSM). TSM is defined as the concentration of total particulate matter, including both, the organic fraction (mostly represented by chlorophyll-*a* – Chl-*a*) and the inorganic fraction (clay, sand and silt) (DEKKER *et al.*, 2001) in water. TSM composition results in distinct spectral responses and can provide specific information on the water composition. Besides spectral features, suspended matter intensively modifies the limnological dynamics of inland waters, as reservoirs and its hydroelectric potential (BILOTTA & BRAZIER, 2008).

Several aquatic systems have been evaluated by using remote sensing data. In the Zhujiang River (near Pearl River), in China, Dazhao *et al.* (2012) used in situ data and Hyperion images to estimate TSM concentrations. Zhujiang River is the main responsible to discharge its suspended solids into Pearl River, and TSM showed a moderated correlation with chlorophyll-a (R^2 = 0.44). The results indicated that near infrared (NIR) spectral interval was the most suitable range in such case to retrieved TSM concentrations.

Band ratio (B4/B1) was used to evaluate the Enhanced Thematic Mapper (ETM^+) sensor on board of Landsat satellite to estimate the suspended matter in the eutrophic Taihu Lake. Taihu Lake is a shallow aquatic system (mean depth around 1.9 meters) and presented algae blooms every year (MA & DAI, 2005). The authors also found a strong correlation between TSM and band 4 (NIR region) / band 1. The use of Moderate Resolution Imaging Spectroradiometer (MODIS) was evaluated by Bi *et al.* (2011), and showed that the band ratio, R_{rs} 645 nm / R_{rs} 555 nm, presented a satisfactory performance for Bohai Strait environment, which is dominate by inorganic compounds, such as silt and clay from Huanghe delta (Yellow River).

Much attention have been devoted to develop models for seawaters, bays, estuaries, lakes, oceans and rivers in order to characterize aquatic environments by using hyper or multi- remote sensing approach, but there are few algorithms available to estimate TSM concentrations in tropical reservoirs. Therefore, studying TSM in hydroelectrical reservoirs, such as Barra Bonita Hydroelectrical Reservoir (BBHR), by using remote sensing data should be explored mainly due to the main advantages of remote sensing approach – reduced cost and achieving synoptic vision when bio-optical models are applied to remote-sensing images.

BBHR's hydroelectric plant is part of the most important Brazilian waterway (Tietê-Parana, responsible to transport 80% of the Brazilian agricultural production (MOREIRA,

2012). In addition, fish biodiversity decreased more than 50% since 1980 (PETESSE & PESTRERE JR., 2012), due to natural and anthropogenic driving forcings, which highlight the relevance of aquatic system monitoring.

Relied on the use of remote sensing data for aquatic compounds estimating by using bio-optical models, the main objective of this study was to investigate the suitability of in situ hyperspectral data to estimate TSM in BBHR.

2. MATERIALS AND METHODS

In order to meet the main goal of this work, limnological and radiometric dataset were collected in BBHR, and the higher correlation between the wavelength and TSM concentrations could be found. Details about the methodology are described in the following topics.

2.1 Study area

This study was conducted in BBHR (Fig. 1), which is part of two watersheds: Middle Tietê and Sorocaba River Basin (UGRHI-10) and Piracicaba, Capivari e Jundiaí rivers Basin (UGRHI-5) (PRADO *et al.*, 2007). BBHR was constructed in 1963, flooding an area of around 324.84 km^2 and it is the first in a series of large reservoirs in cascade in Tietê river (Barra Bonita, Bariri, Ibitinga, Promissão, Nova Avanhandava and Três Irmãos) (TUNDISI, *et al.*, 2008).

For more than 50 years, several researchers described BBHR as a eutrophic environment and attributed this trophic state to its geographical location – near of urban areas (São Paulo state capital and other cities) and receiving their sewage discharges (PRADO & NOVO, 2005; TUNDISI *et al.*, 2008; BUZELLI & CUNHA-SANTINHO, 2013).

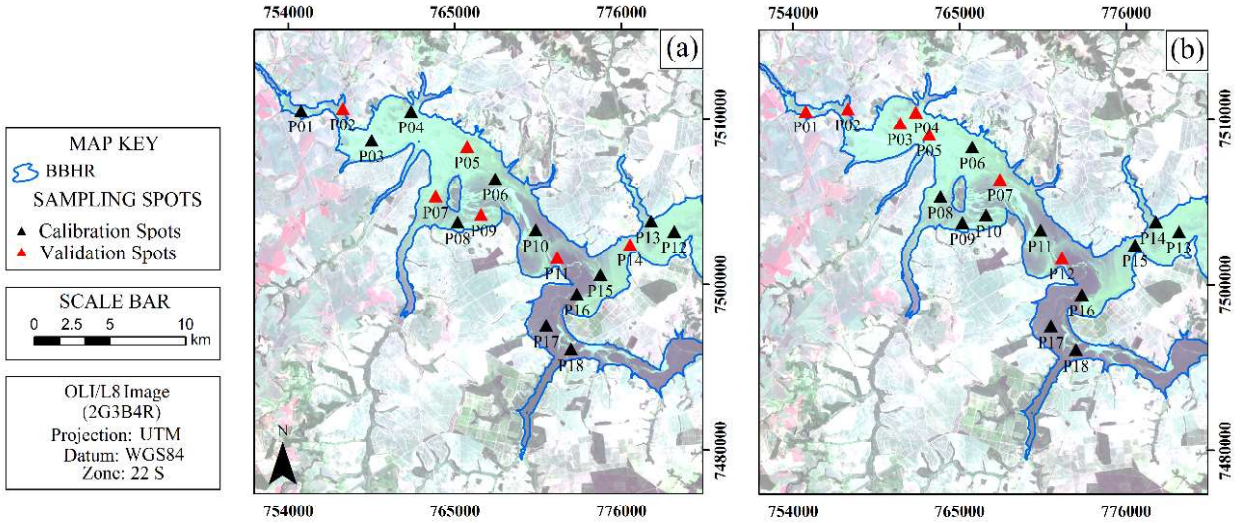

Fig. 1 - Study area (OLI image from 13 October 2014 – 2B3G4R) contained sampling spots collected in (a) May, 2014; and (b) October, 2014. Calibration and validation spots are highlighted.

2.2 Fieldwork

The in situ data were gathered in two field campaigns carried out from 05th to 08th May 2014, and 13th to 16th October 2014, in BBHR. The 36 sampling spots were defined considering a 2014 time-series of Landsat 8 Operational Land Imager (OLI) images from 2014, where the pixels with higher variances were defined as sampling spots to represent temporal and composition changes in BBHR.

Limnological, geographic and radiometric data were measured at each sampling spot during the campaign. The geodetic coordinates were collected by using a Global Navigation Satellite System (GNSS) receptor.

Waters samples were collected at each sampling spot for laboratory determination of TSM and Chl-*a* concentrations. The water samples were collected around 0.3 m below the surface in polyethylene dark bottles, and were preserved in low temperatures until the laboratory analysis (one week later). In the laboratory, TSM concentrations were obtained following the American Public Health Association (APHA) protocol (APHA, 1998). In addition, Secchi

disk depth with Secchi disk (SD - in meters), Dissolved Oxygen (mg.L^{-1}) and turbidity (in NTU) also were measured, both with portable gadgets.

At the same time, the following radiometric measurements were made above the water: total radiance (L_t – W.m².sr^{-1}), diffuse irradiance (L_{sky} – W.m².sr^{-1}), and downwelling irradiance (E_d – W.m²). Radiometric measurements were made at each sampling spot using RAMSES – TriOS hyperspectral radiometers, with 3.3 nm of spectral resolution (from 320 nm to 950 nm) and a field of view of 7º (www.trios.de). Measurements were made with an azimuthal angle of 90° in order to minimize the glint effect (MOBLEY, 1999). Then, the radiometric measurements were used to calculate the R_{rs} (sr^{-1}) following the Eq. (1) (MOBLEY, 1999).

$$R_{rs}(\theta,\varphi,\lambda,0^+) = \frac{L_t(\theta,\varphi,\lambda,0^+) - 0.028 \times L_{sky}(\theta,\varphi,\lambda,0^+)}{E_d(\theta,\varphi,\lambda,0^+)} \quad (1)$$

2.3 Bio-optical models

Empirical models (see Table 1) were selected to estimate TSM in BBHR. The selection of these models was made based on TSM retrieval models published in literature, such as DZ12, MM04, FA14 and AL98. Other models, such as KA06 and JE00 were chosen due to low TSM interval (similar range with TSM concentrations in BBHR). In addition, the models with band ratio were chosen to minimize atmospheric effects (caused by atmospheric compounds), emphasize spectral features and reduce the effects of variable particle grain sizes and sediment refractive indices (MATTHEWS, 2011).

Models were calibrated by using 23 samples among of 36 samples (the remainder 13 samples were used for validation). The samples for calibration and validation were selected based on upper and lower values criteria (ONDERKA & PEKAROVÁ, 2008).

Besides existing models, the Interactive Correlogram Environment (ICE) (OGASHAWARA *et al.*, 2014) was used to speed the selection of ratio, which presented high correlation with TSM. Linear and non-linear models (exponential and 2nd polynomial) were tested to calibrate the models, which are shown in Table 1.

Error analysis was made using Root Mean Squared Error (RMSE, in %), and Mean Absolute Percentage Error (MAPE, in %). Due to quadratic term in Eq. 2, RMSE increase a lot if a single residual is higher than other. However, MAPE indicated the percentage of error and do not have the "quadratic problem" (Eq. 3), then MAPE was not too sensitive to magnitude of residuals. Furthermore, coefficient

Table 1: Summary of remote-sensing algorithms used in this study to retrieve empirical models

ID	Reference	Environment	TSM(mg.L^{-1})		Model
DZ12	Dazhao *et al.* (2012)	Estuary	*9.1	**45.7	$R_{rs}(813\ nm) + \frac{R_{rs}(742\ nm) - R_{rs}(844\ nm)}{2}$
)MM04	Miller and Mckee (2004)	Golf	*0	**<60	$R_{rs}(650\ nm)$
KA06	Kallio *et al.* (2006)	Lakes	*0.7	**32	$R_{rs}(705\ nm)$ - $R_{rs}(714\ nm)$
JE00	Jorgensen and Edelvang (2000)	Ocean	*0	**30	$R_{rs}(544\ nm)$
AL98	Althuis (1998)	Ocean	*1	**45	$R_{rs}(630\ nm)$ - $R_{rs}(750\ nm)$
N-ICE	This paper	Reservoir	*3.6	**32.8	$\frac{R_{rs}(720\ nm)}{R_{rs}(695\ nm)}$

*Minimum and ** Maximum values.

of determination (R^2) was used to evaluate the calibration of models. R^2 indicated the total of variance that could be explained by the model. The schematic methodology used in this study was summarized in Fig.2.

$$\text{RMSE}\ (\%) = \sqrt{\frac{\sum_{i=1}^{n}(x_i - x_{true})^2}{n}} \times \frac{100 \times n}{\sum_{i=1}^{n} x_i} \qquad (2)$$

$$\text{MAPE}\ (\%) = \frac{\sum_{i=1}^{n}|x_i - x_{true}|}{\sum_{i=1}^{n} x_{true}} \times 100 \qquad (3)$$

Where n (=13) is the total of validation sampling spots, x_i represents the estimated values and x_{true} is the measured value in situ (reference data).

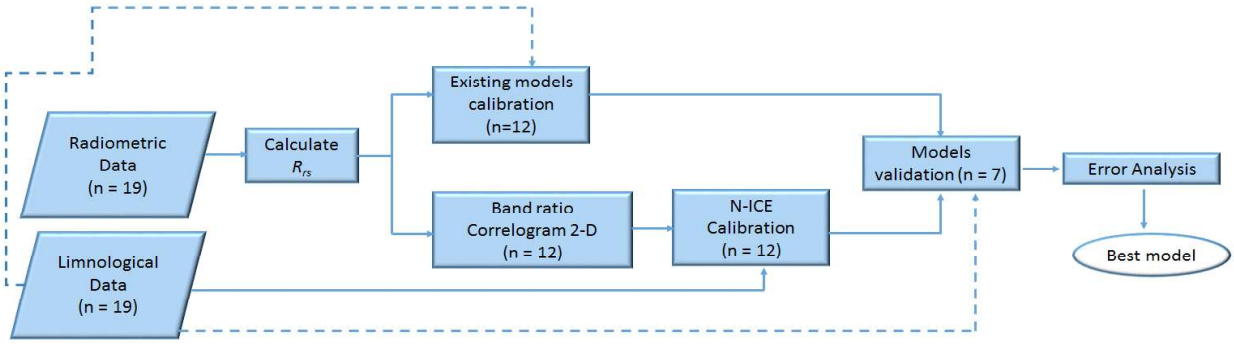

Fig. 2 - Flowchart showing the methodology used in the present work.

3. Results and Discussion

Descriptive statistics for limnological parameters are shown in Table 2. Measured TSM concentrations in BBHR ranged from 3.6 to 32.8 mg.L^{-1}, with a mean of 14.08 mg.L^{-1} and standard deviation of ±8.11 mg.L^{-1}. Upper lowest and highest TSM values were found in P06 and P10 sampling spots in first and second campaign, respectively (see Fig. 1 for location). Higher turbidity levels occurred in the second campaign, which implied in lower SD values (turbidity environments trend to present lower SD values than clearer aquatic systems). Chl-*a* concentration presented the highest coefficient of variation. Expressive Chl-*a* concentration indicated that suspended matter in BBHR is mostly composed by organic fraction (phytoplanktons and its derivatives), and demonstrated the intense metabolic phytoplanktons activities in BBHR.

The R_{rs} spectra collected at some sampling spots are in Fig. 3. There are specific features in the spectral curves, such as chlorophyll absorption features at blue (400 – 500 nm) and red range (600 – 700 nm) owing to the high Chl-*a* concentrations in BBHR. Increasing in

Table 2: Limnological data at each sampling spot (see Fig. 1 for location)

Sampling Spots	TSM (mg.L^{-1})	Chl-*a* (µg.L^{-1})	Dissolved Oxygen (mg.L^{-1})	Secchi Disk (m)	Turbidity. (NTU)
Minimum	3.6	17.75	3.8	0.37	1.66
Maximum	32.8	797.80	15.7	2.3	33.2
Mean	14.07	280.92	9.85	1.05	12.01
Median	11.2	268.39	9.9	0.79	11.6
Standard Deviation	8.11	195.96	3.14	0.56	7.91
Coefficient of variation	58%	70%	32%	53%	66%

TSM concentrations tends to increase R_{rs} values in NIR, as was observed in all sampling spots plotted in Fig. 3. This increase in the NIR range can be explained by the particle scattering in the water. Moreover, there is a peak near 570 nm in all spectral curves. The spectral range from 570 nm to 680 nm can provide information about the nature of suspend solids: in BBHR the presence of absorption features derived from high levels of Chl-*a* characterized the presence of phytoplankton, almost 85% of organic fraction. Though this information can be useful to estimate Chl-*a* concentrations and consequently, BBHR eutrophic state, estimating TSM is more accurate when using R_{rs} in NIR spectral region (RITCHIE *et al.*, 1976).

The lower spectral curve is related to TSM= 4.5 mg.L^{-1} and Chl-*a*=121.23 µg.L^{-1} (in P15, in the first fieldwork), which can be justified owing to the high Chl-*a* absorption. Although spectral curves were influenced by several water compounds (qualitatively and quantitatively), they maintained a spectral shape in all analyzed sampling spots in Fig. 3.

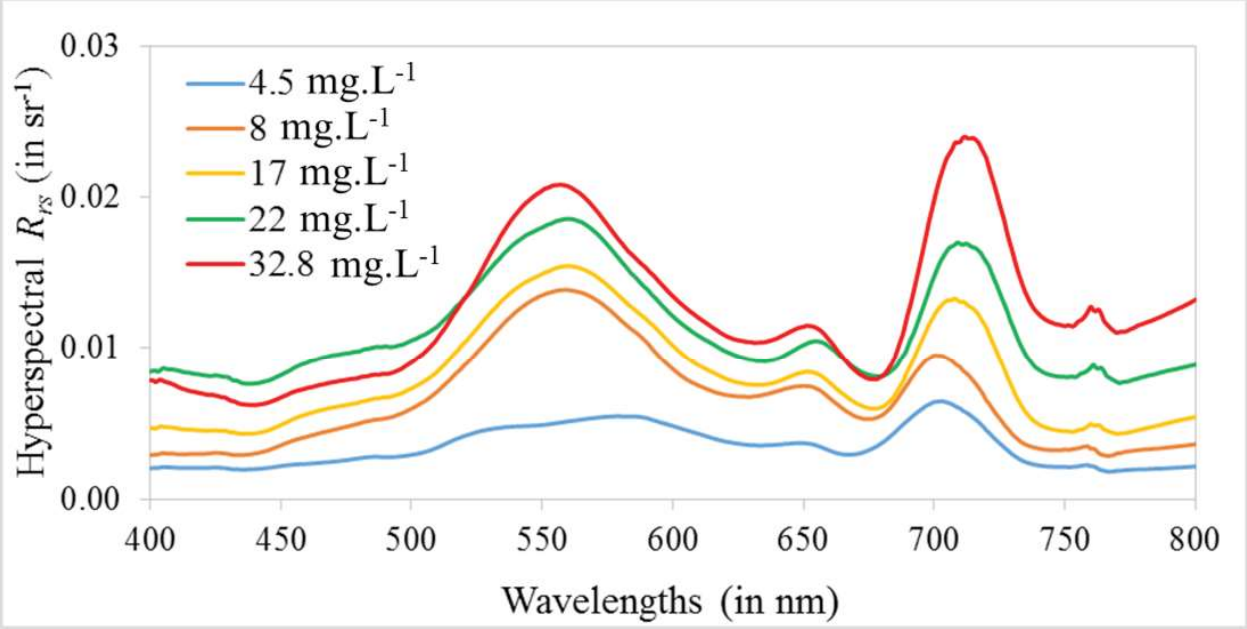

Fig. 3 - Hyperspectral R_{rs} spectrum considering some specific TSM concentrations (mg.L^{-1}) in BBHR.

3.1 Empirical models calibration

Obtained coefficient of correlation (R) from ICE webtool are shown in Fig. 4. The best band ratio (R = 0.94), named N-ICE, consisted in R_{rs} 720 nm over R_{rs} 695 nm. Although was obtained a higher R, there is no physical meaning to explain the band ratio, which is a limitation of methodology of statistical models. All selected bio-optical models (from literature) and N-ICE were calibrated by using linear, exponential and quadratic functions (see Table 3).

In order to demonstrate obtained R^2 by ICE webtool, in situ TSM measurements and N-ICE band ratio was plotted in Fig.4 (b), and showed high relationship for linear, quadratic and exponential fits.

The highest R^2 from a linear fit was 0.89, and the lowest linear fit regression got a R^2 of 0.28, from N-ICE and AL98 models, respectively. DZ12 model also presents a good fit (R^2 = 0.81 in exponential regression adjust). Some models did not adjust very well but it can be explained due to different concentrations, compositions, type grain size and distribution of the suspended matter in Barra Bonita. In order to evaluate the probability of the regression coefficients being significantly different from zero we analyzed the *p-value* (BINDING *et al.*, 2005). Linear, exponential and quadratic models from all models are able to estimate TSM values, once the models were statistically significant considering 1% of significance level.

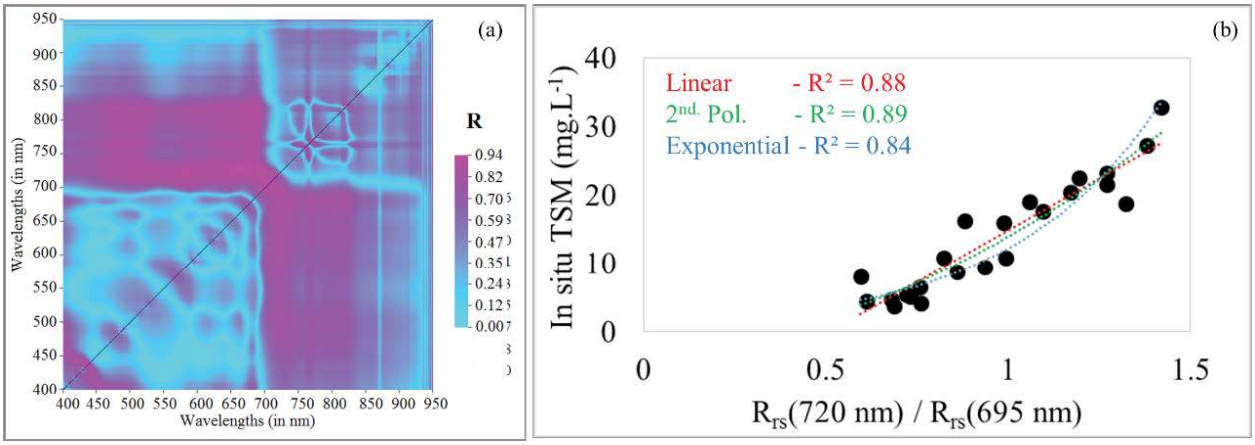

Fig. 4. (a) 2-D color correlation plot by ICE showing correlation coefficient as statistical estimator and the highest R^2 (0.94); (b) Best band ratio (720 nm/ 695 nm) in ICE considering adjustments with in situ TSM measurements (in $mg.L^{-1}$).

Table 3. Calibration parameters of the models

MODEL	ADJUST[a]	*a*	*b*	*c*	*p*-value[b]	R^2
DZ12	Linear	7184.3	4.77	-	<0.001	0.77
	2nd. Pol.	-1E6	12354	1.92	<0.001	0.66
	Exponential	5.72	539.15	-	<0.001	0.81
MM04	Linear	3227.5	-9.04	-	<0.001	0.65
	2nd. Pol.	29365	2796.5	-7.58	<0.001	0.65
	Exponential	1.73	264.55	-	<0.001	0.66
KA06	Linear	-10390	18.07	-	<0.001	0.70
	2nd. Pol.	3E6	-11122	16.78	<0.001	0.72
	Exponential	15.23	-736.5	-	<0.001	0.53
JE00	Linear	1597.5	-4.07	-	<0.001	0.60
	2nd. Pol.	-399455	2566.4	-9.35	<0.001	0.60
	Exponential	2.66	129.03	-	<0.001	0.59
AL98	Linear	-4674.1	23.05	-	0.001	0.39
	2nd. Pol.	7551.48	-67615	23.31	0.016	0.28
	Exponential	21.15	-319	-	0.001	0.41
N-ICE	Linear	30.44	-15.60	-	<0.001	0.88
	2nd. Pol.	13.94	2.56	-2.56	<0.001	0.89
	Exponential	1.10	2.41	-	<0.001	0.84

[a]The configuration of adjusts were $y=ax+b$ (linear); $y=ax^2+bx+c$ (2nd. Pol.); and $y=a.e^{bx}$ (exponential); [b]p-value > 0.05 (indicated that models were not statistically significant)

The NIR and red spectral ranges provided the best models, which can be explained by the shifting of the R_{rs} peak in the NIR and absorption in the red (see Fig. 3). Explanations for the shifting of R_{rs} peak in NIR are related to high Chl-*a* levels that occurred in BBHR owing to phytoplankton bloom formation (characterized by high absorption features in blue/red spectral intervals, and scattering in red/NIR regions). Estimating TSM was possible due to high reflectance in NIR (LODHI *et al.*, 1998), as observed in Fig. 3 for wavelengths more than 700 nm.

3.2 Model validation

To compare the models, scatterplots between the measured and the estimated TSM concentrations, from all models, were plotted (Fig. 5). The best models found were DZ12 and JE00, both with linear regression calibration. Error analysis was performed in order to compare the models and verify which models present better estimates.

Evaluating all values, RMSE ranged between 20.8% (from DZ12) and 64% (from

AL98). MAPE ranged between 22.1% and 74%. The lowest values for MAPE and RMSE indicated that DZ12 and JE00 were able to estimate TSM concentrations accurately. In spite of the great N-ICE determination coefficient of calibration (R^2 = 0.89), the model showed at least a RSME = 26% and MAPE = 31% values, indicating poorest TSM estimates in BBHR when compared to other models.

According to Chen *et al.* (2013), the strong absorption by water in the NIR reduces the recorded signal magnitude, the signal-to-noise ratio, and consequently, enhanced the inherent noise effect in reflectance measurements, which can contribute to TSM retrieval errors, although, JE00 and DZ12 showed lowest RMSE and MAPE for all fits.

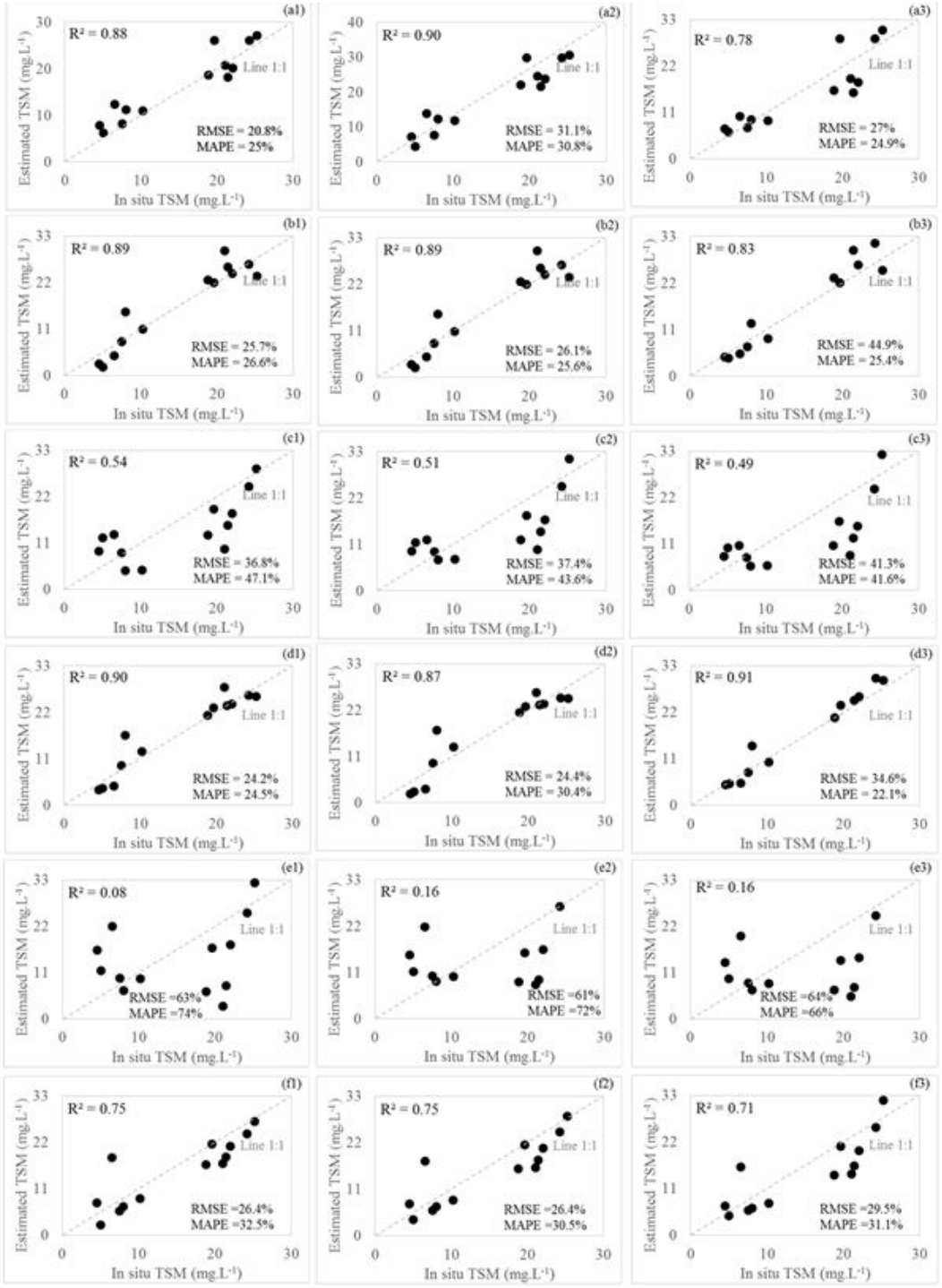

Fig. 5. Estimated *versus* Measured TSM concentrations (in mg.L^{-1}) for Linear (left); 2nd Polynomial (middle); Exponential (right) fits: (a) DZ12 model; (b) RC91 model; (c) N-ICE model, with respective obtained errors.

Obtained results indicated the type of water system is relevant but it was not as important characteristic that affects the result as the sensitive wavelengths for TSM estimates. Such assumption was in DZ12 and JE00 used wavelengths and the presence of reflectance features, which provided better R^2 and lowest errors.

TSM distribution can be achieved applying the best model in a time series of images. Then, considering the best sensor to apply the model DZ12 (NIR spectral range) is a hyperspectral sensor, such was did by Dazhao *et al.*, (2012), which used a Hyperion data. However, the use of JE00 model, in 544 nm, can be applied to spectral images in green interval.

4. Conclusions

The best TSM retrieval model was DZ12 linear model, owing to its lowest error when compared to another assessed algorithms. However, DZ12 model can be applied to hyperspectral images owing to spectral bands used in TSM estimates (742nm, 813 nm, and 844 nm). Considering that the NIR region was the most suitable spectral range to develop TSM retrieval model, further investigations should be made to analyze the suitability of NIR spectral bands onboard MODIS and OLI. Alternatively, JE00 also provided a low error and was developed by using 544 nm (similar to some existing spectral bands at imager-sensors), which can be applied for TSM mapping regions that present similar BBHR features.

Future study will focus on examining the peak and signal shift in NIR with higher TSM concentration, the interaction between other optically active constituents in this spectral region and the model application to satellite images. In addition, the results will be compared to analytical approaches that are going to performed.

ACKNOWLEDGEMENTS

This work was supported by São Paulo Research Foundation (FAPESP) under grant number 2012/19821-1 and Brazilian Council for Scientific and Technological Development (CNPq) under grants 300301/2012-0, 472131/2012-5 and 400881/2013-6. The first author would also thanks the Coordination for the Improvement of Higher Education Personnel (CAPES) for the scholarship.

REFERENCES

ALTHUIS, I. J. A. Suspended Particulate Matter detection in the North Sea by hyperspectral airborne remote sensing. **Aquatic Ecology**, v. 32, p. 93-98, 1998

American Public Health Asociation (APHA), **Standard Methods for the Examination of Water and Wastewater** (Washington, D.C., 2005). A publicação está fora de formatação!

BI, N.; Zousheng, Y.; Wang, H.; Fan, D.; Sun, X.; Lei, K. Seasonal variation of suspended-sediment transport through the southern Bohai Strait. **Estuarine, Coastal and Shelf Science.** V. 93, p. 239-247, 2011.

BILOTTA G. S; BRAZIER R.E. Understanding the influence of suspended solids on water quality and aquatic biota. **Water Research**, v. 42, p. 2849–2861, 2008.

BINDING, C.E., BOWERS, D.G.; MITCHELSON-JACOB, E.G. Estimating suspended sediment concentrations from ocean colour measurements in moderately turbid waters; the impact of variable particle scattering properties. **Remote Sensing of Environment,** v. 94, n. 3, p. 15373–15383, 2005.

BUZELLI, G. M.; CUNHA-SANTINO, M. B. Análise e diagnóstico da qualidade da água e estado trófico do reservatório de Barra Bonita (SP). **Ambi-Agua**, v. 8, n. 1, p. 186-205, 2013.

CHEN, J.; D'SA, E.; CUI, T.; ZHANG, X. A semi-analytical total suspended sediment retrieval model in turbid coastal waters: A case study in Changjiang River Estuary. **Optics Express**, v. 21, n. 11, p. 13018-13031, 2013.

DAZHAO, L.; DONGYANG, F.; BING, X.; CHUNYAN, S. Estimation of total suspended matter in the Zhuijiang (Pearl) River estuary from Hyperion imagery. **Chinese Journal of Oceanology and Limnology**. v. 30, n. 1, p. 16-21, 2012.

DEKKER, A.G. *et al.* Comparison of remote sensing data, model results and in situ data for total suspended matter (TSM) in the southern Frisian lakes. The Science of the Total

Environment, v. 268, p. 197 – 214, 2001.

GOODIN, D.G.; HAN, L.; FRASER, R.N.; RUNDQUIST, D.C.; SCHALLES, J.; STEBBINS, W.A. Analysis of Suspended Solids in Water Using Remotely Sensed High Resolution Derivative Spectra. **Photogrammetric Engineering and Remote Sensing**, v. 59, n. 04, p. 505-510, 1993.

GITELSON, A.; GARBUZOV, G.; SZILAGYI, F.; MITTENZWEY, K-H.; KARNIELI, A.; KAISER, A. Quantitative remote sensing methods for real-time monitoring of inland quality. **International Journal of Remote Sensing**, v. 14, n. 7, p. 1269-1295, 1993.

JORGENSEN, P.V.; EDELVANG, K. CASI data utilized for mapping suspended matter concentrations in sediment plumes and verification of 2-D hydrodynamic modelling. **Interternational Journal of Remote Sensing**, v. 21, n. 11, p. 2247-2258, 2000.

KALLIO, K.; KUTSER, T.; KOPONEN, S.; PULLIAINEN, J.; VEPSÄLÄINEN, J.; PYHÄLAHTI, T. Retrieval of water quality from airborne imaging spectrometry of various lake types in different seasons. **The Science of the Total Environment**, v. 268, p. 59–77, 2001.

LODHI, M.A.; RUNDQUIST, D.C.; HAN, L.; KUZILA, M. Estimation of Suspended Sediment Concentration in Water Using Integrated Surface Reflectance. **Geocarto International**. v. 13, n. 2, p. 11-15,1998.

MA, R.; DAI. J. Investigation of chlorophyll-a and total suspended matter concentrations using Landsat ETM and field spectral measurement in Taihu Lake, China. **International Journal of Remote Sensing**, v. 26, n. 13, p. 2779-2787, 2005.

MATTHEWS, M.W. A current review of empirical procedures of remote sensing in inland and near-coastal transitional waters. **International Journal of Remote Sensing**, v. 32, n. 21, p. 6855-6899, 2011.

MILLER, R. L.; MCKEE, B. A. Using MODIS Terra 250 m imagery to map concentrations of total suspended matter in coastal waters. **Remote Sensing of Environment**, v. 93, p. 259–266, 2004.

MOBLEY, C.D. Estimation of the remote-sensing reflectance from above-surface measurements. **Applied Optics**, v. 38, n. 36, p. 7442-7455, 1999.

MOREIRA, M. C. A. **Avaliação da influência da barragem de Barra Bonita – SP na morfodinâmica do rio Tietê e seus impactos à navegação**. Dissertação (Mestrado em Engenharia Civil). Programa de Pós-Graduação em Engenharia Civil. Universidade Estadual de Campinas – Unicamp, Campinas. 99 p. 2012.

ODERMATT, D.; GITELSON, A.; BRANDO, V.E.; SCHAEPMAN, M. Review of constituent retrieval in optically deep and complex waters from satellite imagery. **Remote Sensing of Environment**, v. 118, p. 116-126. 2012.

OGASHAWARA, I.; CURTARELLI, M.P.; SOUZA, A.F.; AUGUSTO-SILVA, P. B.; ALCÂNTARA, E.H.; STECH, J.L. Interactive Correlation Environment (ICE) – A Statistical Web Tool for Data Collineatiry Analysis. **Remote Sensing**. v. 6, p. 3059-3074, 2014.

ONDERKÁ, M.; PEKAROVÁ, P. Retrieval of suspended particulate matter concentrations in the Danube River from Landsat ETM data. **Science of the total environment.** v. 397, n. 2, p. 238-243, 2008.

PETESSE, M.L.; PETRERE Jr, M. Tendency towards homogenization in fish assemblages in the cascade reservoir system of the Tietê river basin, Brazil. **Ecological engineering**, v. 48, p. 109-116, 2012.

PRADO, R. B; NOVO, E. M. L. M. Aplicação de geotecnologias na modelagem do potencial poluidor das sub-bacias de contribuição para o reservatório de Barra Bonita - SP relacionado à qualidade da água. **Anais**... In: XII Simpósio Brasileiro de Sensoriamento Remoto, Goiânia, Brasil, INPE, p. 3253-3260, 2005.

PRADO, R. B.; NOVO, E.M.L.M.; PEREIRA, M. N. Avaliação da dinâmica do uso e cobertura da terra na bacia hidrográfica de contribuição para o reservatório de Barra Bonita - SP. **Revista Brasileira de Cartografia**. v. 59, n. 2, p. 127-135, 2007.

RITCHIE J. C.; SHIEBE, F.R.; McHENRY, J.R. Remote sensing of suspended sediment in surface water. **Photogram. Eng. Remote**

Sensing, v. 42, p. 1539–1545, 1976.

ROTTA, L. H. S.; IMAI, N.N.; BOSCHI, L.S.; BATISTA, L.F.A. Imagem de alta resolução especial na detecção de macrófitas submersas – estudo de caso. **Revista Brasileira de Cartografia**, v. 65, n. 1, p. 95-109, 2013.

TANG, S.; LAROUCHE, P. NIEMI, A.; MICHEL, C. Regional algorithms for remote-sensing estimates of total suspended matter in the Beaufort Sea. **International Journal of Remote Sensing**. v. 34, n. 19, p. 6562-6576, 2013.

TUNDISI, J.G.; MATSURA-TUNDISI, T.; ABE, D.S. The ecological dynamics of Barra Bonita (Tietê River, SP, Brazil) reservoir: implications for its biodiversity. **Brazilian. Journal of Biology**, 68(4, Suppl.), p. 1079-1098, 2008.

VOLPE, V.; SILVESTRI, S.; MARANI, M. Remote sensing retrieval of suspended sediment concentration in shallow Waters**. Remote Sensing of Environment**, v. 115, p. 44–54, 2011.